Hu *et al. Biology Direct* (2024) 19:82
https://doi.org/10.1186/s13062-024-00532-8

Biology Direct

RESEARCH Open Access

# ARMCX1 inhibits lung adenocarcinoma progression by recruiting FBXW7 for c-Myc degradation

Zhe Hu[1†], Yilin Wu[2†], Xiaoou Sun[3], Yanli Tong[4], Houkuang Qiu[5] and Enqing Zhuo[1*]

## Abstract

**Background** Armadillo Repeat Containing X-Linked 1 (ARMCX1), a member of the ARM Repeat X-linked protein family, exerts inhibitory function in various tumors. However, its biological role in lung adenocarcinoma (LUAD) and the underlying molecular mechanisms require further exploration.

**Methods** LUAD tissue microarrays and bioinformatic databases were used to evaluate the relationship between ARMCX1 and clinicopathological features. The influence of ARMCX1 on LUAD cell proliferation, migration, and invasion in vitro was determined by colony formation, CCK-8, EdU incorporation, cell cycle, wound healing, and Transwell assays. The impact of ARMCX1 on LUAD cell growth and metastasis in vivo was determined by subcutaneously transplanted tumor and pulmonary metastasis assays. Western blot, immunoprecipitation, immunofluorescence, cycloheximide, and proteasome inhibitor assays were finally conducted to explore the potential underlying molecular mechanisms.

**Results** ARMCX1 expression was downregulated in clinical LUAD samples due to which patient prognoses were poor. Functional experiments indicated that ARMCX1 overexpression inhibited the growth and metastasis of LUAD cells in vitro and in vivo. The molecular mechanism suggested that ARMCX1 recruits the E3 ubiquitin ligase FBXW7 for mediating ubiquitinated degradation of c-Myc, suppressing its nuclear accumulation, and ultimately inactivating cell cycle and epithelial-mesenchymal transition (EMT) signals.

**Conclusion** ARMCX1 inhibits LUAD cell proliferation and metastasis by interacting with c-Myc and enhancing its ubiquitination and degradation. Consequently, it can act as a tumor suppressor in this disease. These results suggest that ARMCX1 is a potential target in the treatment of LUAD.

**Keywords** ARMCX1, c-Myc, FBXW7, Lung adenocarcinoma, Tumor suppressor, Ubiquitination

[†]Zhe Hu and Yilin Wu contributed equally to this work.

*Correspondence:
Enqing Zhuo
eqing009@163.com
[1]Department of Second Ward Oncology, The Affiliated Guangdong Second Provincial General Hospital of Jinan University, Guangzhou 510317, China
[2]Department of Cardiology, The Affiliated Guangdong Second Provincial General Hospital of Jinan University, Guangzhou 510317, China
[3]Institute of Biomedical and Pharmaceutical Sciences, Guangdong University of Technology, Guangzhou 510006, China
[4]Department of Pharmacy, The Affiliated Guangdong Second Provincial General Hospital of Jinan University, Guangzhou 510317, China
[5]Department of Laboratory Medicine, The Affiliated Guangdong Second Provincial General Hospital of Jinan University, Guangzhou 510317, China

## Background

The predominant histological subtype of lung cancer, a very deadly malignant tumor globally, is lung adenocarcinoma (LUAD) [1–3], and its therapy has entered the "precision medicine" era. For patients with specific gene mutations or positivity, such as epidermal growth factor receptor (EGFR) mutations in NSCLC, targeted EGFR tyrosine kinase inhibitors improve therapeutic outcomes and result in longer median progression-free survival than conventional chemotherapy [4]. Moreover, for patients with anaplastic lymphoma kinase-positive NSCLC, adjuvant treatment with alectinib significantly reduces the risk of disease recurrence or death compared to that with chemotherapy [5]. Therefore, identifying novel significant biomarkers is crucial for diagnosing and treating LUAD.

The ARMCX gene family is found on the X chromosome and contains armadillo (ARM) repeat sequences. This family of proteins has been demonstrated to play a vital role in a number of important biological functions, such as organelle and intercellular cascade reactions [6], thermogenic adipose tissue plasticity [6], neural differentiation [7], and hepatic tumorigenesis [8]. ARMCX1, also known as ALEX1, is a member of the ARM repeat X-chain of proteins, which contains an important N-terminal transmembrane structural and two ARM repeat sequences. The gene encoding this protein is closely localized on the X chromosome with other members of the family, including *ARMCX2* and *ARMCX3*. ARMCX1 modulates mitochondrial translocation and kinetic functions, attenuates traumatic brain injury, and exerts a neuroprotective effect [9–11]. In cancer research, early studies reported that *ARMCX1* transcripts were lost or that mRNA levels were reduced in various tumors [12]. Subsequent studies in colorectal and pancreatic cancer cells revealed that mutations in the key cis-regulatory element of *ARMCX1* impair the function of the *ARMCX1* promoter [13]. The *ARMCX1* promoter is highly methylated, which inhibits colony formation of colorectal cancer cells and negatively regulates breast cancer cell proliferation [14, 15]. Furthermore, gastric cancer tissues and cells contain a highly methylated ARMCX1 promoter, and overexpression of ARMCX1 suppresses gastric cancer cell growth and metastasis [16].

c-Myc is one of the most frequently activated oncogenic transcription factors, and numerous studies have reported that it modulates the cell cycle, apoptosis, metabolism, adhesion, and protein synthesis by regulating a wide array of genes [17–21]. Furthermore, c-Myc expression is often aberrant in most tumors and involved in cell proliferation, migration, invasion, and ositinib resistance in LUAD [22–24]. Notably, c-Myc is a highly unstable protein, with its stability regulated by ubiquitination and deubiquitination. It is one of the key targets of the E3 ubiquitin ligase FBXW7 [25, 26].

However, the biological role of ARMCX1 in LUAD and the underlying molecular mechanisms are not well understood. In this study, we revealed that ARMCX1 expression is abnormally downregulated in LUAD compared to that in the normal epithelium and that it correlates with a poorer prognosis in patients. The proposed molecular mechanism involves an ARMCX1 interaction with c-Myc, promoting the ubiquitin-mediated degradation of the latter through FBXW7 recruitment, ultimately inhibiting LUAD proliferation and metastasis. In summary, we investigated the effects of ARMCX1 on LUAD progression and the underlying molecular mechanisms. These findings provide a theoretical basis for the use of ARMCX1 as a potential target for the treatment of LUAD.

## Materials and methods

### Tissue samples and immunohistochemistry

The LUAD microarray (HLugA180Su08, Outdo Biotech, Shanghai, China) was used for immunohistochemistry (IHC) staining scoring. Visualization of the staining signals in the microarray was achieved using the streptavidin/peroxidase and DAB kits (ZSGB BIO). A score > 6 represented high expression, whereas a score ≤ 6 represented low expression.

### Cell culture

The LUAD cell lines used in this study were H1299, A549, H1975, PC9, and 16HBE. RPMI 1640 (Vivacell, China) containing 10% fetal bovine serum (FBS; Nobimpex, Germany) was used to culture LUAD cells, whereas 16HBE cells were cultured in Dulbecco's modified Eagle medium (Vivacell) with 10% FBS (Nobimpex, Germany). All cell lines were maintained in a humidified chamber at 37 °C with 5% $CO_2$.

### Reverse transcription-quantitative PCR

We extracted total RNA through the Cell Total RNA Isolation Kit (Foregene, China) following the experiment's manual. We then converted mRNA to cDNA via the Reverse Transcription Kit (AG, China), and the cDNA was amplified by adding specific primers. SYBR Green (AG, China) and cDNA were then mixed for qPCR detection. The $2^{-\Delta\Delta Ct}$ assay was applied to evaluated the mRNA level of genes. The primers are displayed in Supplementary Table S1.

### Cell counting Kit-8 (CCK-8) assay

Following the seeding of 2000 LUAD cells into 96-well dishes, 10 μL of Cell Counting Kit-8 (CCK-8) reagent (Vazyme, China) was added for 100 min in a 100 μL system, and a Multiskan Sky Full-wavelength Enzyme

Labeler was used to measure each well's optical density at 450 nm. Cell viability was recorded from days 0 to 4.

### 5-Ethynyl-2'-deoxyuridine incorporation analysis

The 5-Ethynyl-2'-deoxyuridine (EdU) assay was carried out using a Cell-Light EdU Apollo 567 kit (RiboBio, Guangzhou, China), according to the manufacturer's instructions. After co-culturing LUAD cells with EdU A solution for 2 h, the cells were fixed with 4% paraformaldehyde, permeabilized with 0.5% Triton X-100 and then colored with Apollo fluorescent dye and DAPI.

### Colony formation and cell cycle analyses

Three hundred cells per well of stable transfected LUAD cells were injected into 6-well plates, and the media was replaced every 72 h throughout the 12-day incubation period. After incubation, the colonies were stained with crystal violet for 5 min after being fixed for 20 min with 4% paraformaldehyde. As instructed in the experiment handbook, cell cycle analysis was carried out using the Cell Cycle Kit (Leagene, China).

### Wound healing assay

When LUAD cells reached confluency greater than 95% in 6-well plates, a linear scratch wound was made using a 1 mL pipette tip for the wound healing assay. At 0 and 48 h, the decrease in wound width was viewed under a microscope, and pictures were taken.

### Migration and invasion assays

The ability of LUAD cell to migrate and invade was assessed using a Transwell chamber. To this end, $1\times10^5$ LUAD cells were seeded in the Transwell chamber's top chamber after being combined with 100 μL of serum-free RPMI 1640, either with or without BD Matrigel (Corning, USA). In contrast, 10% FBS-supplemented RPMI-1640 was applied to the bottom chamber. Following the specified incubation time, cells on the membrane's bottom were fixed for 20 min with 4% paraformaldehyde dyed with Giemsa (Nanjing JianCheng Technology) for 5 min, and observed under a microscope. Three randomly selected fields of view were taken from each membrane, and Image Pro Plus was implemented to determine the average number of migratory or invading cells in membrane.

### Coimmunoprecipitation

LUAD cells were subjected to immunoprecipitation (IP) lysis, and the cell lysates were treated for an evening at 4 °C with 5 μg of either a particular antibody or normal immunoglobulin G (IgG) using a rotator. The antigen–antibody complexes were then co-incubated with A/G magnetic beads (Bimake, Shanghai) for 60 min at 37 °C. The magnetic beads were cleaned five times with a washing buffer, and 5 × SDS buffer was added to the precipitated compounds; they were boiled for 10 min and analyzed using Western blot.

### Immunofluorescence staining

Following 48 h of plasmid transfection, LUAD cells were inoculated into cultivation plates (Sorfa Life Science, Zhejiang, China). Following a PBS wash, the cells were fixed with 4% paraformaldehyde, permeabilized with 0.5% Triton X-100, and then treated overnight at 4 °C with the appropriate primary antibodies. After that, the cells were stained with second antibodies that were fluorescently tagged, and the cell nuclei were dyed with DAPI.

### Western blot analysis

Standard procedures were utilized for Western blot. Proteintech provided the antibodies against the following: FBXW7 (552901-AP), c-Myc (10828-1-AP), CCND1 (60186-1-Ig), ARMCX1 (20193-1-AP), P21 (10355-1-AP), Vimentin (10366-1-AP), and Ubiquitin (10201-2-AP). E-cadherin (#14472) and N-cadherin (#13116) were acquired from Cell Signaling Technologies, anti-FLAG (F1804) was acquired from Sigma-Aldrich (St. Louis, MO, USA), and anti-GAPDH (AP0063) was obtained from Bioworld. Primary antibodies were diluted using common antibody Dilution Buffer (EpiZyme, Shanghai, China).

### Lentivirus infection and cell transfection

A lentivirus was created using full-length human ARMCX1 and fluorescent protein (GFP) gene sequences (OBIO Technology, Shanghai, China). LUAD cells were infected with an empty GFP vector lentivirus (LV-NC) or an ARMCX1 GFP vector lentivirus (LV-ARMCX1) to generate ARMCX1 stable overexpression clones. RiboBio Lnc generated small interfering RNAs (siRNAs) that selectively target the ARMCX1 gene (Guangzhou, China; Supplementary Table S2). The *ARMCX1* plasmid was synthesized by Weizhou Biosciences Inc. (Shandong, China). Following the manufacturer's instructions, Lipofectamine TM 3000 (Invitrogen) was employed to transiently transfect plasmids or siRNAs into LUAD cells. Cells with treatment were utilized for the subsequent phase of the experiment after 24 to 48 h.

### Animal experiment

Tumor growth was assessed in a subcutaneous xenograft nude mouse model. Female nude mice, aged four weeks, were acquired from Ruige Biology (Guangzhou, China) and maintained in a designated pathogen-free environment. The left and right dorsums of the nude mice were injected with negative control cells and A549 cells ($5\times10^6$) that were stable overexpressors of ARMCX1,

respectively. Every 6 days, the tumor volume was measured. Nude mice were euthanized after 40 days, and the subcutaneous graft tumor tissue was harvested and weighed. In the lung metastasis model, A549 cells ($2\times10^6$) were injected into the tail vein of a nude mice. After 30 days, the nude mice were euthanized, and the lung tissue was removed and photographed under an animal fluorescence microscope. The animal experiments in this study were conducted in accordance with the review of the Institutional Animal Care and Use Committee (IACUC) of Ruige Biotechnology, which is in line with the principles of animal protection, animal welfare, and ethics and complies with the relevant national regulations on the welfare and ethics of laboratory animals.

### Cycloheximide chase and ubiquitination assays

After seeding an equivalent quantity of cells onto 6-well plates, the cells were cultured in a 2 mL system containing cycloheximide (CHX; concentration of 50 μg/ml; Selleck, China). Cells were harvested at different time points for protein extraction and subsequent Western blot experiments. For ubiquitin experiments, LUAD cells were exposed to MG132 at a concentration of 20 μM for 4 h. Cells were treated with IP lysate buffer and extracted, and cell lysates were immunoprecipitated using an anti-c-Myc antibody, then incubated with magnetic beads, and washed four times. Finally, the proteins boiled for 10 min after adding SDS loading buffer, and used for Western blot.

### Statistical analysis

Student's *t*-tests were employed to compare two groups, and one-way analysis of variance was performed to evaluate differences among several groups. The GraphPad Prism 8 software and SPSS Statistics 25 were applied for the statistical analyses. The log-rank test was utilized to assess the survival curve. The Cox regression model was applied to filter prognostic variables that were single or multiple. Statistical significance was established at $p<0.05$.

## Results

### Downregulation of ARMCX1 expression in LUAD is associated with poor patient prognosis

Using the Gene Expression Omnibus (GEO), Cancer Genome Atlas (TCGA), and UALCAN databases, we first examined the expression of ARMCX1 in tumors and normal tissues to determine its involvement in the development of LUAD. In comparison to normal lung tissues, the expression of ARMCX1 was reduced in lung cancer tissues (Fig. 1a-c). Using the KM Plotter database, survival curves were produced, indicating that LUAD patients with high ARMCX1 expression had a greater survival rate than those with low ARMCX1 expression (Fig. 1d). Moreover, using qPCR and Western blot, we found that the mRNA and protein levels of ARMCX1 were downregulated in LUAD cell lines compared to those in normal bronchial epithelial cells (Fig. 1e, f). Immunohistochemical staining and statistical analysis of tissue microarrays further indicated that ARMCX1 expression was markedly decreased in LUAD (Table 1; Fig. 1g). The correlation between ARMCX1 expression and clinicopathological features in LUAD patients was further examined; ARMCX1 expression was significantly correlated with the T, N, and AJCC stages (Table 2). Furthermore, the Kaplan-Meier curve demonstrated that LUAD patients with a low ARMCX1 level had a lower survival time, as compared to that with high ARMCX1 level (Fig. 1h). The T, N, and AJCC stages and ARMCX1 expression were associated with LUAD patient survival based on univariate regression analysis (Fig. 1i). Multivariate regression analysis demonstrated that ARMCX1 expression was an independent predictor of overall survival (Fig. 1j). These results indicate that patients with low ARMCX1 expression have a worse survival probability than those with high expression, which could be closely associated with LUAD progression.

### ARMCX1 overexpression inhibits LUAD cell proliferation, migration, and invasion in vitro

To establish the functional involvement of ARMCX1 in the development of LUAD, we employed Gene Set Enrichment Analysis (GSEA), The findings demonstrated that low ARMCX1 levels have highly enriched genes associated with the cell cycle (Fig. 2a). Based on the low expression of ARMCX1 in most LUAD cells, an ARMCX1 plasmid or lentivirus was used to treat H1299, H1975, and A549 cells, siRNA was utilized to silence ARMCX1 levels in cells stably overexpressing ARMCX1. The impact of ARMCX1 on cell proliferation was then examined using assays for colony formation, CCK-8, and EdU incorporation. Here, overexpression of ARMCX1 considerably inhibited the growth and viability of H1299, H1975, and A549 cells compared to the control group (Fig. 2b-d). Moreover, flow cytometry was employed to ascertain the impact of ARMCX1 on the phase of G1/S; compared to control cells, the portion of G1 phase cells was higher in LUAD cells overexpressing ARMCX1, whereas the proportion of S phase cells was lower (Fig. 2e).

The impact of ARMCX1 in LUAD cells on migration and invasion was examined utilizing Transwell and Wound healing assays. Overexpression of ARMCX1 dramatically suppressed LUAD cell capacity to migrate relative to control cells; it also reduced the quantity of migratory and invasive cells in the Transwell chambers (Fig. 3a-f). Western blot analysis revealed that ARMCX1 overexpression contributed to the downregulation of

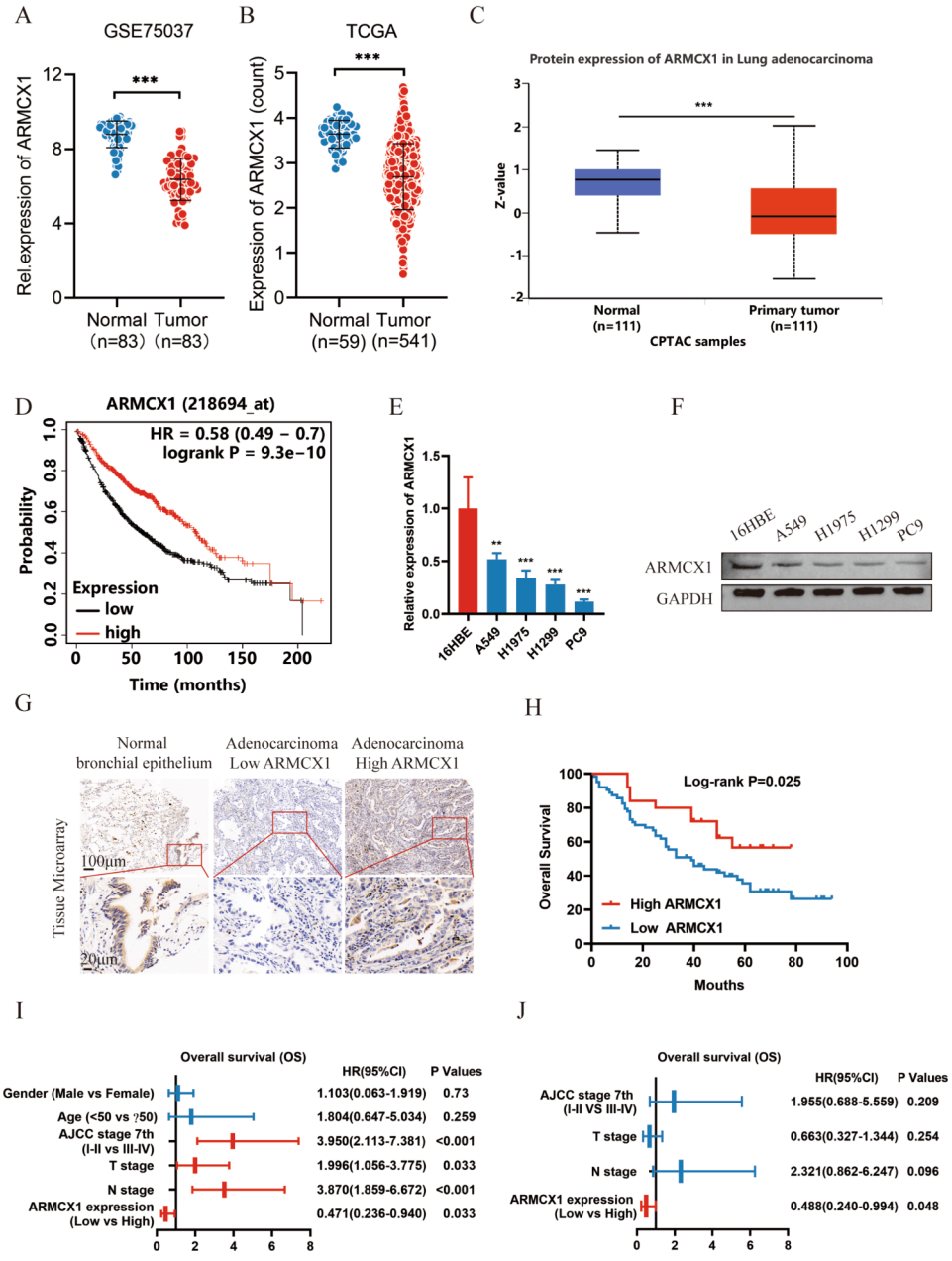


**Fig. 1** ARMCX1 expression is downregulated in LUAD and associated with poor patient prognosis. (**a**-**c**) The expression level of ARMCX1 was analyzed using TCGA, GEO, and UALCAN databases for LUAD. (**d**) The survival curve based on ARMCX1 expression was analyzed using the KM plotter database for LUAD. (**e**, **f**) The mRNA and protein expression levels of ARMCX1 were detected via qPCR and Western blot using 16HBE, H1975, H1299, A549, and PC9 cell lines. (**g**) Representative images generated from tissue microarray immunohistochemistry demonstrate the expression of the ARMCX1 protein (magnification, scale bar: 20 μm). (**h**) Survival curve based on LUAD patients' tissue microarray ARMCX1 expression. (**i**, **j**) Cox regression analysis, both univariate and multivariate, of the clinicopathologic features of LUAD patients

**Table 1** Expression of ARMCX1 in LUAD compared to para-carcinoma tissues

| Group | Cases(n) | ARMCX1 expression | | X2 value | P value |
|---|---|---|---|---|---|
| | | Low | High | | |
| Tumor | 88 | 63 | 25 | 5.784 | 0.016 |
| Normal | 15 | 6 | 9 | | |

**Table 2** Relation between clinicopathologic characteristics and ARMCX1 expression in LUAD

| Factors | | n | ARMCX1 expression | | $X^2$ | P value |
|---|---|---|---|---|---|---|
| | | | Low | High | | |
| Age(y) | < 50 | 10 | 7 | 3 | 0.014 | 0.905 |
| | ≥ 50 | 78 | 56 | 22 | | |
| Gender | Male | 52 | 37 | 15 | 0.011 | 0.913 |
| | Female | 36 | 26 | 10 | | |
| Clinical stage* | I-II | 48 | 29 | 19 | 8.874 | 0.002 |
| | III-IV | 27 | 25 | 2 | | |
| T stage* | T1-T2 | 65 | 43 | 22 | 4.292 | 0.038 |
| | T3-T4 | 20 | 18 | 2 | | |
| N stage* | N0-N1 | 55 | 36 | 19 | 4.383 | 0.036 |
| | N2-N3 | 20 | 18 | 2 | | |

*Some patients are not included in the statistics owing to the missing data

the oncogenic c-Myc and the cell cycle-related protein CCDN1. Furthermore, after ARMCX1 overexpression, protein levels of the mesenchymal marker N-cadherin and Vimentin were downregulated, whereas the epithelial marker E-cadherin and cell cycle-related protein P21 were upregulated (Fig. 3g).

Conversely, after silencing ARMCX1, the proliferation of H1299 and A549 cells was increased (Fig. 4a, b, and d), and the migratory and invasive capacities were enhanced (Fig. 4c, e, f, and g). Moreover, the expression of c-Myc, CCND1, and N-cadherin was elevated when ARMCX1 was silenced, whereas the expression of E-cadherin and P21 was decreased in LUAD cells (Fig. 4h). These results indicated that ARMCX1 is crucial to the biological functions performed by LUAD cells.

### ARMCX1 overexpression attenuates LUAD cell tumorigenicity and metastasis in vivo

To elucidate the biological roles of ARMCX1 in vivo. we utilized subcutaneously implanted tumors and lung metastasis models. Nude mice were divided into two groups based on A549 cells: a negative control group and a stable ARMCX1-overexpressing A549 cell group. Subcutaneous implants of control ($5\times10^6$) and stable ARMCX1-overexpressing A549 ($5\times10^6$) cells were made in the left and right backs, respectively (Fig. 5a). After 40 days, nude mice were euthanized, and subcutaneously transplanted tumor nodules were harvested. The weights and volumes of tumor nodules in the ARMCX1-overexpressing group were decreased compared to control group (Fig. 5b). IHC staining discovered that, compared to the control group, the level of ARMCX1 was higher and the level of Ki-67 was downregulated in the ARMCX1-overexpressing group (Fig. 5c). We further injected A549 cells ($2\times10^6$) into the tail veins of naked mice to establish a lung metastasis model (Fig. 5d). The green fluorescence signal associated with lung metastases in the ARMCX1-overexpressing group was markedly attenuated compared to the control group (Fig. 5e).

### ARMCX1 interacts with c-Myc

After confirming that ARMCX1 inhibits the proliferation and metastasis of LUAD, the underlying mechanisms that underlie the inhibitory effects of ARMCX1 on the advancement of LUAD were explored in more detail. The BioGRID protein database was used to predict putative proteins that might interact with ARMCX1. The results suggested that ARMCX1 might bind c-Myc. Co-IP and immunofluorescence staining were used to analyze the interactive relationship between these two proteins. The results suggested that ARMCX1 binds to and co-localizes with c-Myc (Fig. 6a, b, e). Notably, ARMCX1 overexpression inhibited c-Myc nuclear accumulation (Fig. 6g). FBXW7 tightly regulates the degradation of tumor proteins, which is induced by the proteasome system, and is a vital tumor suppressor. Nevertheless, c-Myc is one of its target proteins, and overexpression of ARMCX1 was found to downregulate c-Myc protein level. Therefore, we examined the relationship among ARMCX1, c-Myc, and FBXW7 expression. Co-IP and immunofluorescence staining demonstrated that ARMCX1 binds to and co-localizes with FBXW7 (Fig. 6c, d, f). In summary, ARMCX1, c-Myc, and FBXW7 interact with each other.

### ARMCX1 promotes ubiquitination and degradation of c-Myc through FBXW7 recruitment

In the previous experiments, we confirmed the interaction among ARMCX1, c-Myc, and FBXW7. Also, ARMCX1 negatively modulates c-Myc protein levels. However, the GEO (GSE75037) database analysis indicated no correlation between the mRNA levels of ARMCX1 and c-Myc/FBXW7 in LUAD tissue (Fig. 7a). Furthermore, qPCR experiments indicated that the overexpression of ARMCX1 does not modulate *c-Myc* mRNA levels in LUAD cells (Fig. 7b). We thus speculated that ARMCX1 might enhance c-Myc degradation by the recruiting FBXW7. Following a 4 h treatment with the proteasome inhibitor MG132, the reduction in c-Myc induced by ARMCX1 overexpression was restored

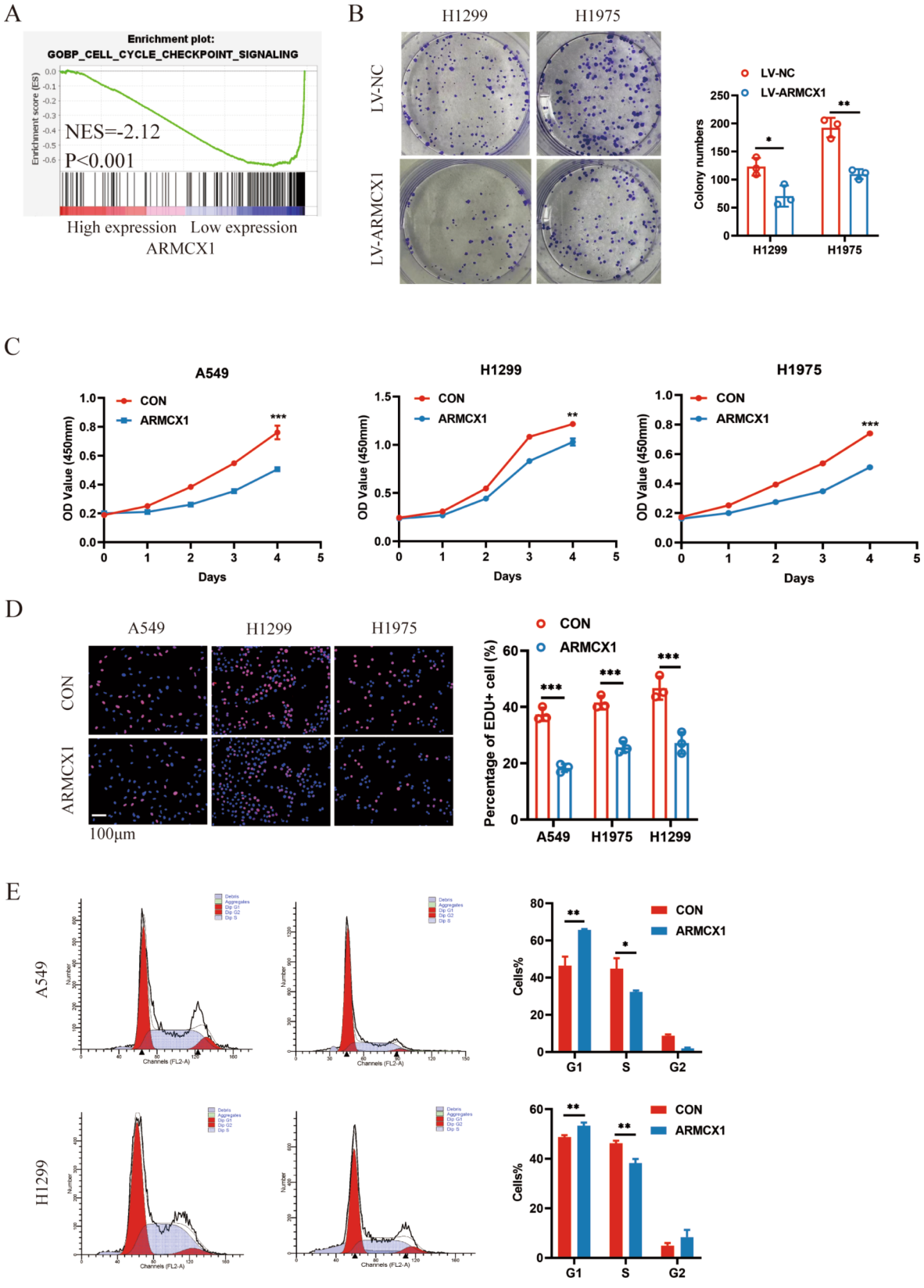


**Fig. 2** ARMCX1 inhibits LUAD cell proliferation. (**a**) GSEA revealed that cell cycle-related signals were significantly enriched with low expression levels of ARMCX1. (**b**) Colony formation, (**c**) CCK-8, and (**d**) EdU incorporation (Scale bar: 100 μm) assays were conducted to evaluate the effect of ARMCX1 on cell proliferation in LUAD cells. (**e**) Flow cytometric analysis of the cell cycle was employed to assess the impact of ARMCX1 on LUAD cell G1/S transition. Mean ± SD, *$p < 0.05$, **$p < 0.01$, ***$p < 0.001$

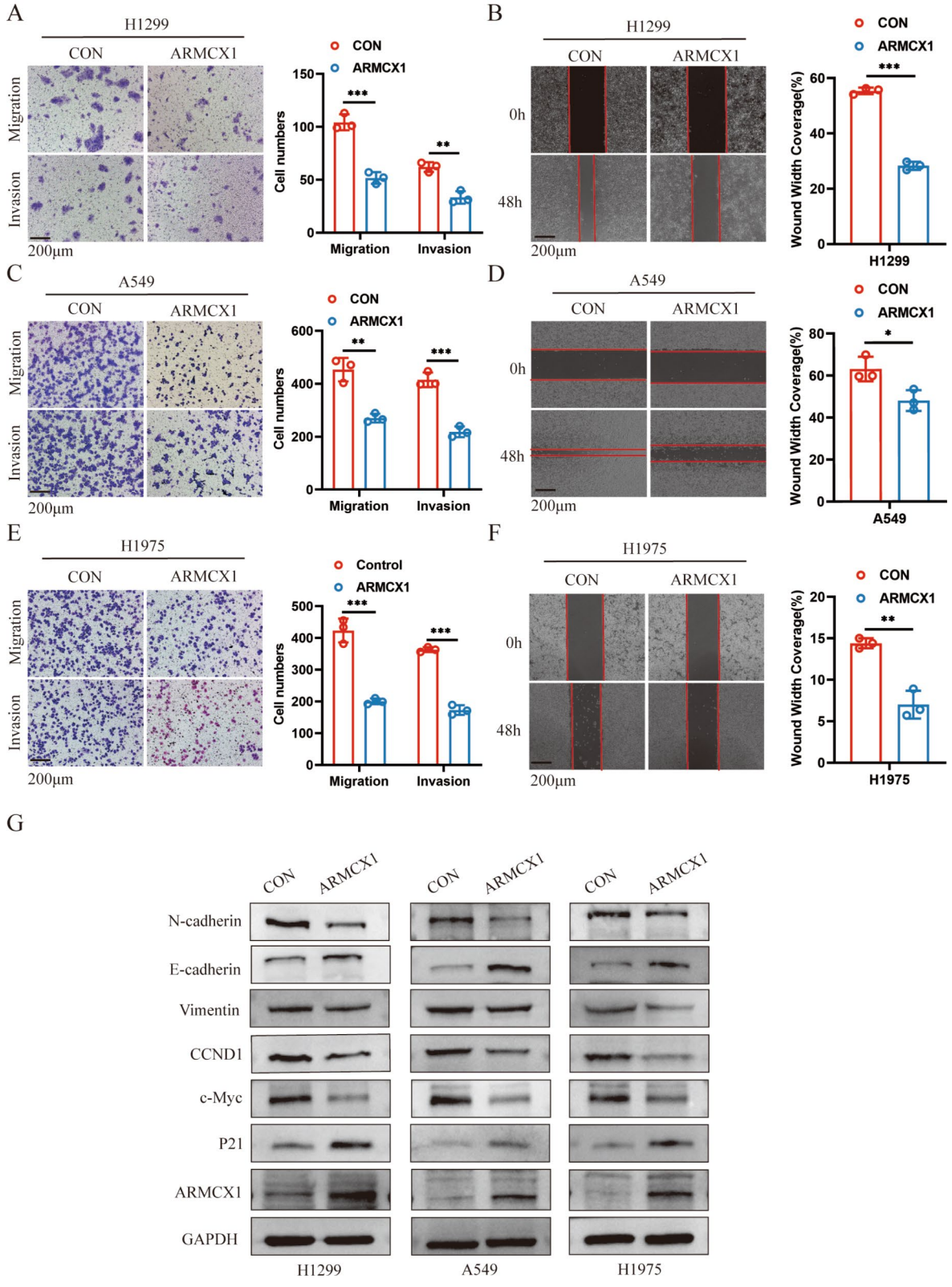


**Fig. 3** ARMCX1 inhibits LUAD cell migration and invasion. (**a**-**f**) Wound healing and Transwell assays (Scale bar: 200 μm) to verify the effect of ARMCX1 on LUAD cell migration and invasion. (**g**) Western blot was employed to assess N-cadherin, E-cadherin, vimentin, CCND1, c-Myc, P21, and ARMCX1 protein levels in control and ARMCX1-overexpressing LUAD cells. Mean ± SD, $^{*}p < 0.05$, $^{**}p < 0.01$, $^{***}p < 0.001$

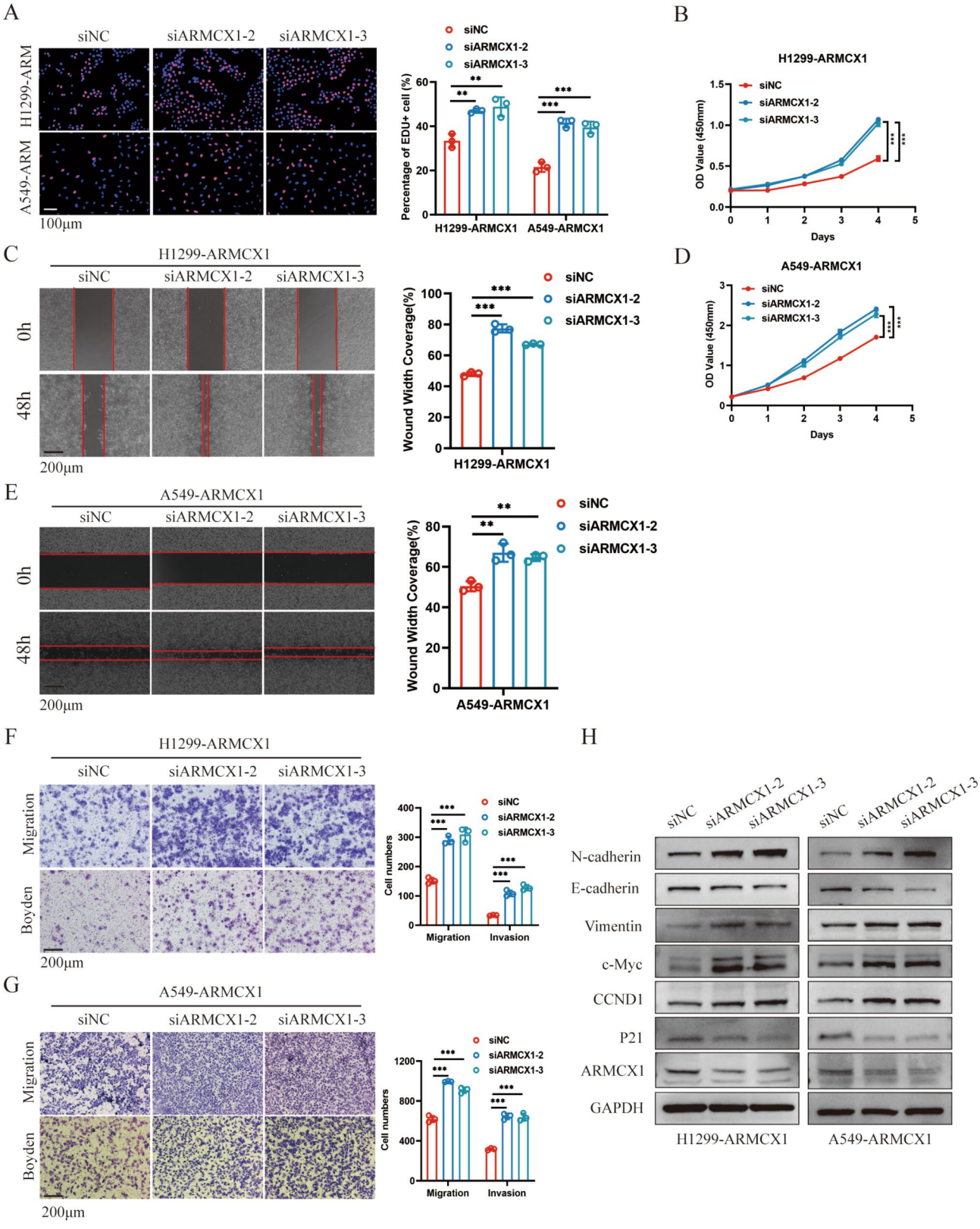


**Fig. 4** ARMCX1 knockdown promotes LUAD cell proliferation, migration, and invasion. (**a**) EdU incorporation, (**b**, **d**) CCK-8, (**c**, **e**) wound healing, and (**f**, **g**) Transwell assays were performed after transfecting siNC, siARMCX1-2, or siARMCX1-3 into ARMCX1-overexpressing LUAD cells. (**h**) Western blot was performed to evaluate N-cadherin, E-cadherin, vimentin, CCND1, c-Myc, P21, and ARMCX1 protein changes after transfecting siNC, siARMCX1-2, or siARMCX1-3 into ARMCX1-overexpressing LUAD cells. Mean ± SD, $^{**}p < 0.01$, $^{***}p < 0.001$

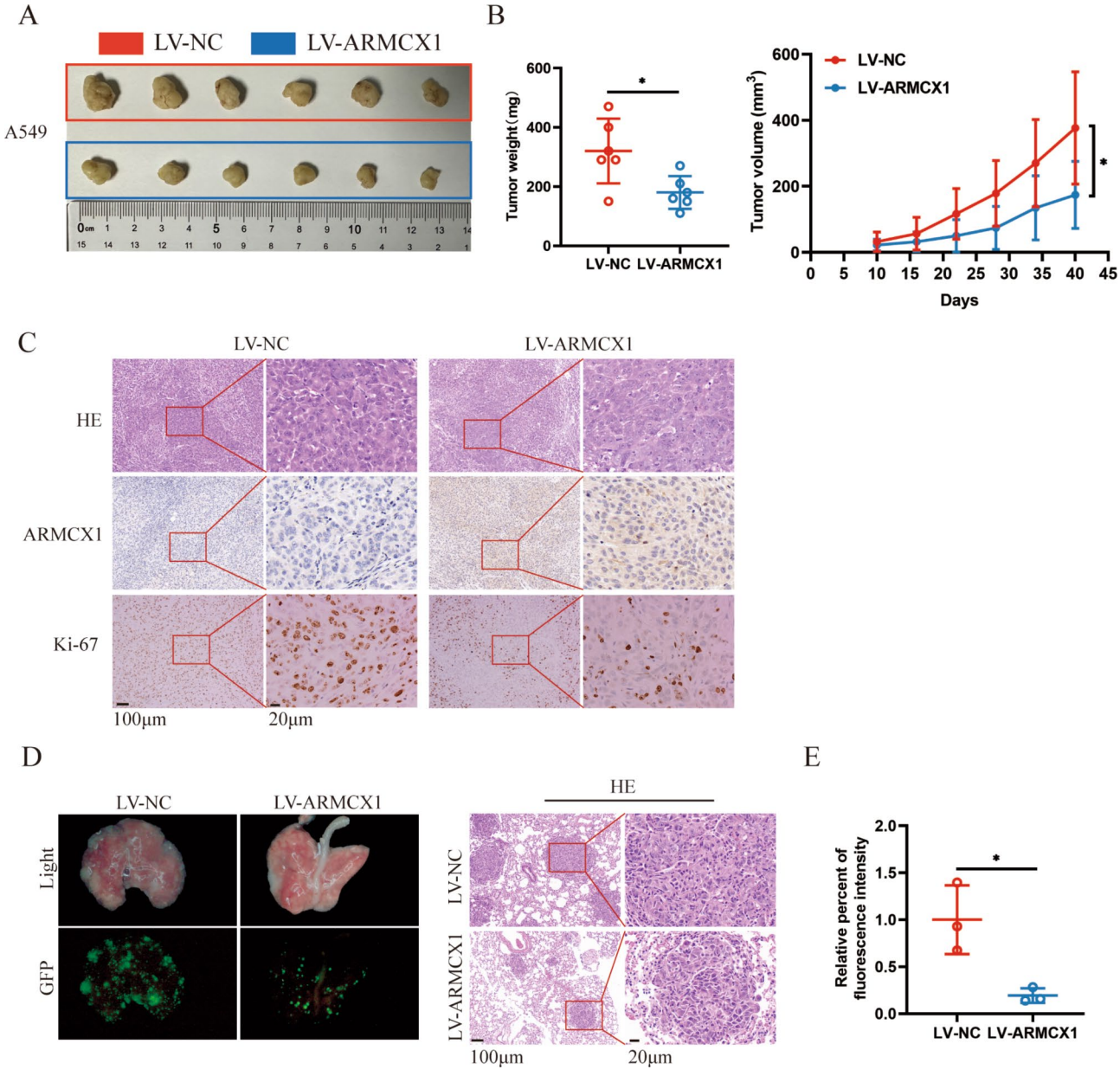


**Fig. 5** ARMCX1 overexpression attenuates LUAD cell tumorigenicity and metastasis. (**a**) Tumors from stable ARMCX1-overexpressing and control A549 cells. (**b**) Weight and volume curves of tumors generated from stable ARMCX1-overexpressing and control A549 cells. (**c**) Representative HE, Ki67, and ARMCX1 immunohistochemical staining of tumor tissues derived from LV-NC and LV-ARMCX1 A549 cells. (**d**) Representative HE staining of lung tissue from the LV-NC and LV-ARMCX1 groups (magnification, scale bar: 20 μm). (**e**) Fluorescence intensity of lung tissues from cells stably overexpressing ARMCX1 and control A549 cells

(Fig. 7c, d). Moreover, a CHX chase test was performed to identify alterations in the half-life of c-Myc resulting from ARMCX1 overexpression. Compared to that in control LUAD cells, ARMCX1 overexpression shortened the half-life of the c-Myc protein (Fig. 7e-h). Subsequently, Western blot showed upregulation of c-Myc after FBXW7 knockdown in ARMCX1 overexpression cells (Fig. 7i), immunoprecipitation revealed that ARMCX1 enhanced c-Myc degradation, and this trend was reversed by silencing FBXW7 (Fig. 7j, k). These results demonstrate that ARMCX1 promotes the c-Myc degradation via recruiting FBXW7.

(**a**) Correlation of mRNA expression between ARMCX1 and c-Myc/FBXW7. (**b**) The mRNA level of c-Myc after ARMCX1 overexpression. (**c**, **d**) LUAD cells with or without ARMCX1 overexpression were treated with MG132 (20 μM) for 4 h. (**e**, **g**) Western blot to detect the c-Myc half-life in ARMCX1-overexpressing and control LUAD cells treated with cycloheximide (CHX; 50 μg/mL). (**f**, **h**) Curves showing the half-life of the c-Myc

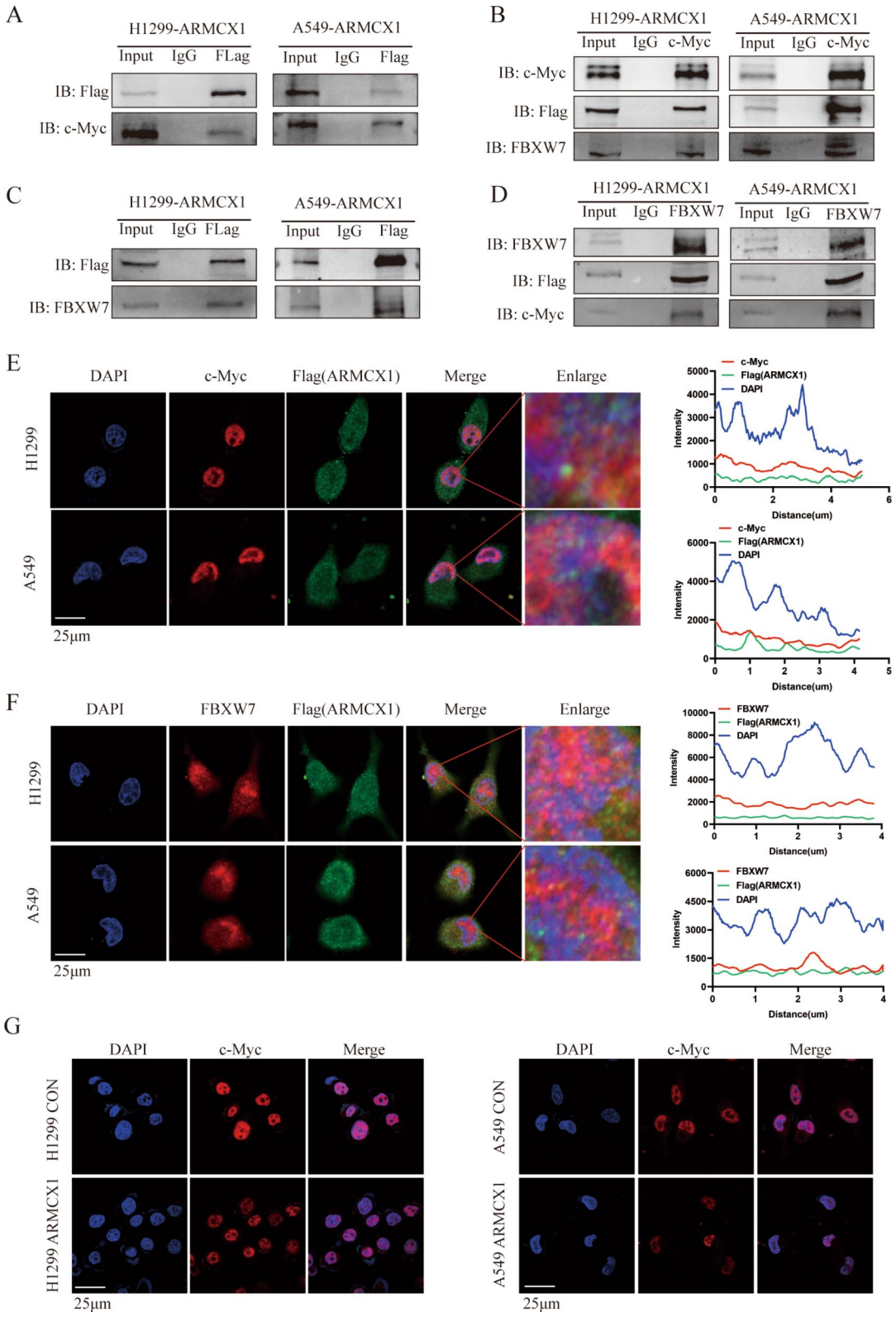


**Fig. 6** ARMCX1 interacts with c-Myc. (**a**, **b**) Co-IP assay of the interaction between ARMCX1 and c-Myc. (**c**, **d**) Co-IP assay of the interaction between ARMCX1 and FBXW7. (**e**) Colocalization of ARMCX1 and c-Myc was detected via immunofluorescence (scale bar: 25 μm). (**f**) Colocalization of ARMCX1 and FBXW7 was detected via immunofluorescence. (**g**) Immunofluorescence staining showed that ARMCX1 suppressed the nuclear accumulation of c-Myc

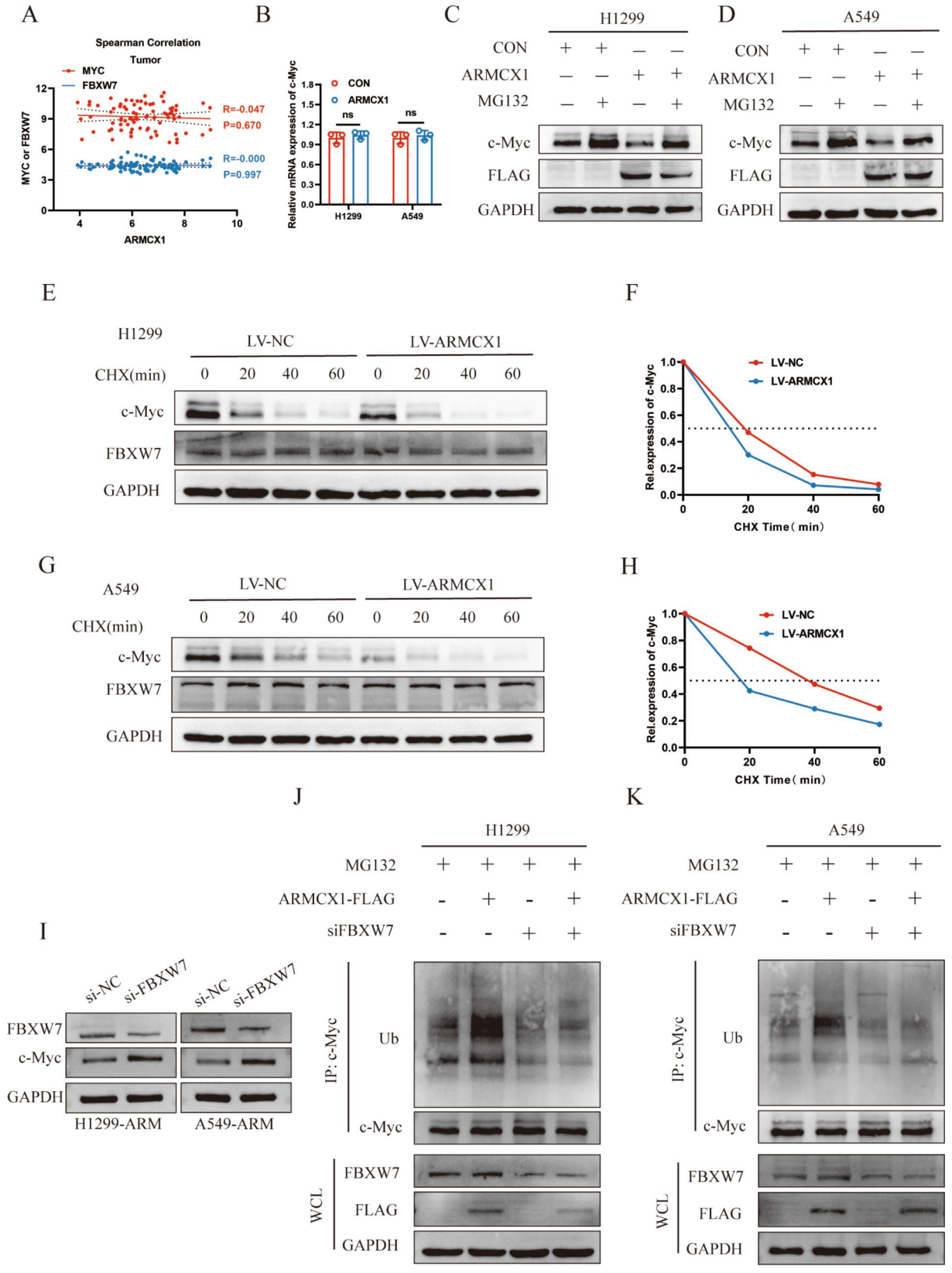


**Fig. 7** ARMCX1 promotes ubiquitination and degradation of c-Myc through FBXW7 recruitment

protein in ARMCX1-overexpressing and control LUAD cells. (**i**) Changes in c-Myc expression after FBXW7 knockdown in ARMCX1-overexpressing cells were analyzed via Western blot. (**j**, **k**) Co-IP and Western blot assays analyzed the impact of ARMCX1 overexpression and siFBXW7 on c-Myc ubiquitination levels.

### c-Myc restores the suppressive impact of ARMCX1 overexpression on LUAD cell proliferation, migration, and invasion

To further clarify the function of c-Myc in ARMCX1-modulated LUAD phenotypes, we introduced a c-Myc plasmid into cells that overexpressed ARMCX1. Subsequent EDU, Transwell and Boyden assays revealed that c-Myc upregulation restored the impacts on cell proliferation, migration, and invasion induced by ARMCX1 overexpression (Fig. 8a-c). Moreover, c-Myc overexpression diminished the inhibitory effects of ARMCX1 overexpression on the protein expression of N-cadherin, vimentin, CCND1, and c-Myc (Fig. 8d). In conclusion, this study demonstrates that ARMCX1 is a tumor suppressor of LUAD that inhibits c-Myc-induced cell cycle progression and EMT signaling by recruiting FBXW7 to degrade c-Myc.

## Discussion

It has been demonstrated that ARMCX1 functions as a cancer suppressor in gastric and colorectal malignancies [14, 16]. However, the underlying molecular mechanisms and the biological role of ARMCX1 in LUAD remain unclear. In the current study, based on the TCGA, GEO, and UALCAN databases, we discovered that LUAD tissues express less ARMCX1 compared to normal lung tissues. Moreover, our in vitro findings utilizing cell lines demonstrated that, in comparison to normal bronchial epithelial cells, ARMCX1 protein expression was frequently downregulated in LUAD cell lines, which matched the predictions in the database. The Kaplan–Meier plotter database suggested that LUAD patients with lower ARMCX1 expression have a poorer survival rate, which was consistent with our tissue microarray survival analyses, which suggested that decreased ARMCX1 results in a poorer prognosis for LUAD patients. Cox regression analysis further discovered that ARMCX1 is an independent prognostic factor for LUAD patients. These data provide evidence for the tumor-suppressive role of ARMCX1 in LUAD.

Interestingly, in experiments based on biological functions, we discovered that ARMCX1 overexpression inhibits the proliferation, migration, and invasion of LUAD cells, whereas ARMCX1 inhibition has the reverse effect. In addition, the results from the nude mouse xenograft and lung metastasis models further validated the in vivo inhibitory effect of ARMCX1 on proliferation and metastasis. This is consistent with the suppressive effects of ARMCX1 on breast, gastric, and colorectal cancers. However, in this study, our sample size of lung metastasis model mice was not large enough, which may have led to limited representativeness of the sample. In future studies using the same model, we will increase the sample size to reduce individual differences, thereby improving experimental soundness and reliability.

Epithelial–mesenchymal transition (EMT) is involved in changes in cell adhesion, cytoskeletal rearrangements, embryonic development, and tissue renewal. Moreover, it has a well-established critical function in cancer progression, invasion, metastasis, stemness, immunotherapy, and resistance to chemotherapeutic drugs [27–32]. The present study revealed that the expression of E-cadherin was elevated and that of vimentin and N-cadherin reduced following ARMCX1 overexpression, whereas this trend was reversed after ARMCX1 silencing, which agrees with the findings of research into gastric cancer [16].

Key cell cycle regulators modulate the growth and development of tumors [33]. c-Myc and CCND1 are essential pro-oncogenic factors involved in the cell cycle; one target that c-Myc modulates to hasten the pace at which cells transition from the G1 to S phase is CCND1, which eventually triggers cell cycle dysfunction [34–37]. Furthermore, in the Wnt signaling pathway, c-Myc and CCND1 are direct downstream targets of the β-catenin-TCF/LEF complex, and these proteins are activated when cells become cancerous. Finally, this promotes β-catenin to translocate to the nucleus and link itself to the TCF/LEF factor to induces high expression of c-Myc and CCND1, which consequently modulates cell cycle and EMT signals [38]. In this study, we found that c-Myc and CCND1 were downregulated and that P21 expression was upregulated after ARMCX1 overexpression, whereas this trend was reversed after ARMCX1 silencing.

To delve into the molecular processes via which ARMCX1 influences LUAD progression, we used the BioGRID database to screen for candidate ARMCX1-interacting proteins and validated the results using Co-IP and immunofluorescence assays. We found that c-Myc interacts and co-localizes with ARMCX1 in LUAD cells. We further explored the regulatory relationship between ARMCX1 and c-Myc and demonstrated that ARMCX1 overexpression promotes c-Myc degradation. The stability of the exceedingly unstable protein c-Myc is modulated by both ubiquitination and deubiquitination, and it is one of the major targets of the E3 ubiquitin ligase FBXW7. FBXW7 is an important tumor-suppressive protein, and its expression is downregulated in numerous tumors [39–43]; moreover, it promotes the degradation of numerous proteins, such as c-Myc [44, 45]. We experimentally confirmed that ARMCX1 interacts and co-localizes with FBXW7 in LUAD cells. Therefore, we

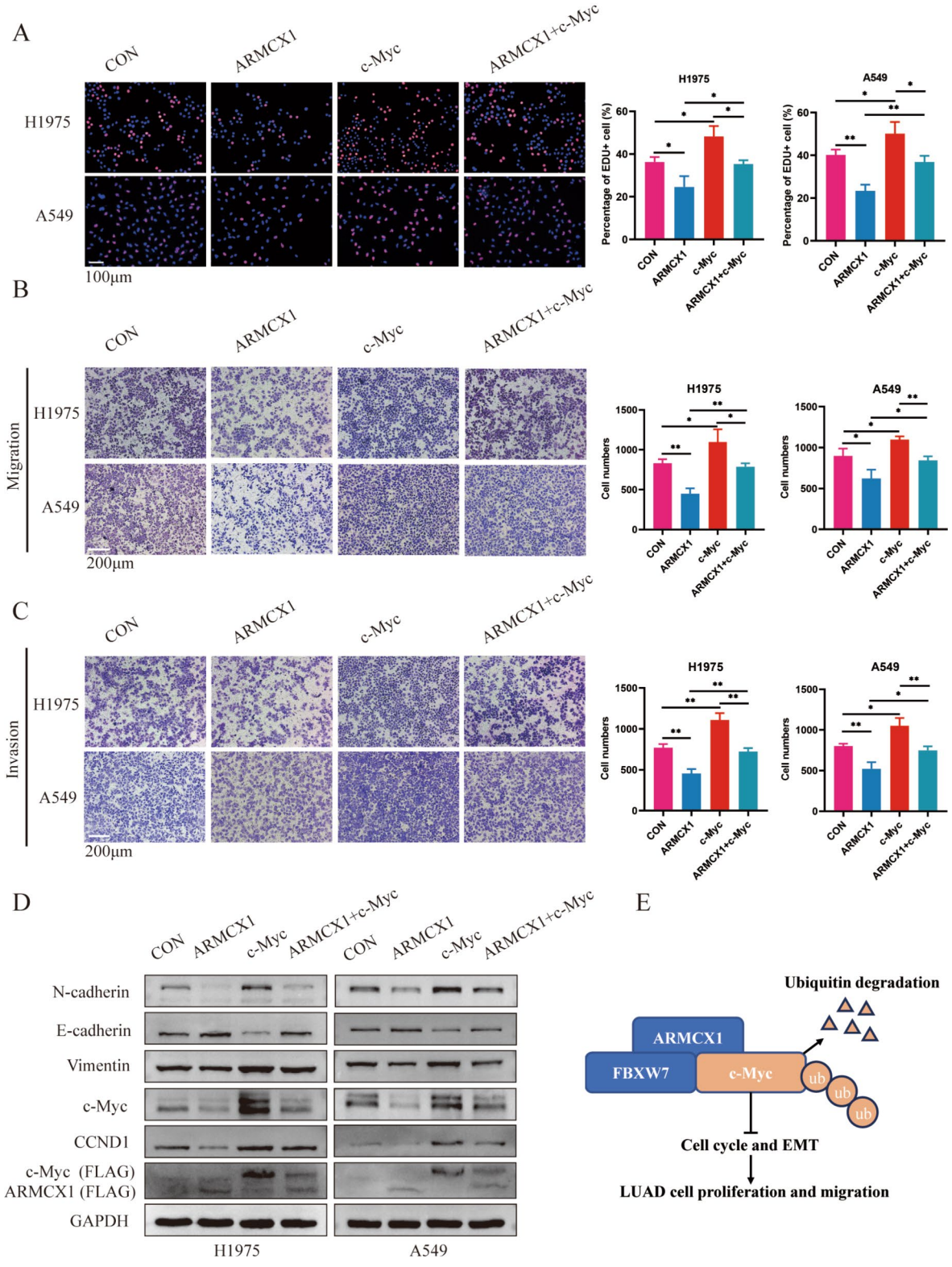


**Fig. 8** c-Myc restores the suppressive impact of ARMCX1 overexpression on LUAD cell proliferation, migration, and invasion. The impacts of c-Myc on the proliferation, migration, and invasion of H1975 and A549 cells overexpressing ARMCX1 were examined by performing EdU incorporation (**a**), Transwell (**b**), and Boyden (**c**) assays. The impacts of c-Myc upregulation on the protein levels of N-cadherin, vimentin, CCND1, E-cadherin, and c-Myc in overexpressed ARMCX1 cells were determined via Western blot (**d**). Mean ± SD, $*p < 0.05$, $**p < 0.01$. (**e**) Diagram illustrating the current study's findings

hypothesized that ARMCX1 recruits FBXW7 to ubiquitinate c-Myc for degradation. Further experimental data showed that FBXW7 mediates c-Myc degradation upon ARMCX1 overexpression.

## Conclusions

We demonstrated that that ARMCX1 expression was lowered in LUAD and that low expression is predictive of a worse outcome for patients. Experiments conducted both in vivo and in vitro revealed that ARMCX1 inhibits LUAD growth and metastasis. Mechanistic studies further suggested that ARMCX1 recruits the E3 ubiquitin ligase FBXW7 to ubiquitinate c-Myc for degradation, thereby suppressing cell cycle progression and EMT signals. This study demonstrated that ARMCX1 is a tumor suppressor in LUAD that inhibits c-Myc-induced cell cycle progression and EMT signaling through the recruitment of FBXW7. These results suggest that ARMCX1 could be targeted for the treatment of LUAD.

### Abbreviations

| | |
|---|---|
| LUAD | Lung adenocarcinoma |
| ARMCX1 | ARM repeat X-chain 1 |
| TCGA | The Cancer Genome Atlas |
| GEO | Gene Expression Omnibus |
| GSEA | Gene Set Enrichment Analysis |
| IHC | immunohistochemistry |
| qPCR | quantitative PCR |
| CCK-8 | Cell Counting Kit-8 |
| EDU | 5-ethynyl-2′-deoxyuridine (EdU) incorporation |
| Co-IP | co-immunoprecipitation |
| EMT | epithelial–mesenchymal transition |

## Supplementary Information

The online version contains supplementary material available at https://doi.org/10.1186/s13062-024-00532-8.

Supplementary Material 1

Supplementary Material 2

### Acknowledgements

We appreciate the Integrated Hospital of Traditional Chinese Medicine of Southern Medical University for providing the experimental equipment and assistance.

### Author contributions

HZ and WYL designed and conducted the main experiments and analyzed the data. HZ and WYL wrote the manuscript. XO S, YL T, and HK Q completed the partial experiments and analyzed the data. EQ Z conceived the study, reviewed the data, and supervised all aspects. All authors read and approved the final manuscript.

### Funding

This study was supported by the Guangzhou Municipal (Academy) Enterprise Joint Key Projects (2023A03J0882) and Guangzhou Municipal Science and Technology Project (2024A03J1058).

### Data availability

No datasets were generated or analysed during the current study.

## Declarations

### Ethics approval and consent to participate

The Institutional Animal Care and Use Committee's (IACUC) of Ruige Biotechnology evaluation was followed when conducting the animal studies for this work, which adhered to the pertinent national rules on the welfare and ethics of laboratory animals and were consistent with the values of animal protection, welfare, and ethics.

### Consent for publication

Not applicable.

### Competing interests

The authors declare no competing interests.

Received: 8 July 2024 / Accepted: 9 September 2024
Published online: 16 September 2024

### References

1. Sung H, Ferlay J, Siegel R, Laversanne M, Soerjomataram I, Jemal A, et al. Global Cancer statistics 2020: GLOBOCAN estimates of incidence and Mortality Worldwide for 36 cancers in 185 countries. CA Cancer J Clin. 2021;71(3):209–49.
2. Molina J, Yang P, Cassivi S, Schild S, Adjei A. Non-small cell lung cancer: epidemiology, risk factors, treatment, and survivorship. Mayo Clin Proc. 2008;83(5):584–94.
3. Herbst R, Morgensztern D, Boshoff C. The biology and management of non-small cell lung cancer. Nature. 2018;553(7689):446–54.
4. Mok T, Wu Y-L, Ahn M-J, Garassino M, Kim H, Ramalingam S, et al. Osimertinib or Platinum-Pemetrexed in EGFR T790M-Positive Lung Cancer. N Engl J Med. 2017;376(7):629–40.
5. Yi-Long W, Rafal D, Jin Seok A, Fabrice B, Makoto N, Dae Ho L et al. Alectinib in Resected ALK-Positive non-small-cell Lung Cancer. N Engl J Med. 2024;390.
6. Mou Z, Tapper A, Gardner P. The armadillo repeat-containing protein, ARMCX3, physically and functionally interacts with the developmental regulatory factor Sox10. J Biol Chem. 2009;284(20):13629–40.
7. Mirra S, Ulloa F, Gutierrez-Vallejo I, Martì E, Soriano E. Function of Armcx3 and Armc10/SVH genes in the regulation of progenitor proliferation and neural differentiation in the Chicken spinal cord. Front Cell Neurosci. 2016;10:47.
8. Mirra S, Gavaldà-Navarro A, Manso Y, Higuera M, Serrat R, Salcedo M et al. ARMCX3 mediates susceptibility to hepatic tumorigenesis promoted by Dietary Lipotoxicity. Cancers (Basel). 2021;13(5).
9. Dengfeng L, Yi W, Guangjie L, Shixin W, Aojie D, Zongqi W et al. Armcx1 attenuates secondary brain injury in an experimental traumatic brain injury model in male mice by alleviating mitochondrial dysfunction and neuronal cell death. Neurobiol Dis. 2023;184.
10. Qiuying L, Haibo N, Qin R, Jiasheng D, Xianghu K, Xugang K et al. Armcx1 reduces neurological damage Via a mitochondrial transport pathway involving Miro1 after traumatic brain Injury. Neuroscience. 2024;545.
11. Romain C, Michael WN, Fengfeng B, Chen W, Siwei L, Yiling Z et al. The mammalian-specific protein Armcx1 regulates mitochondrial transport during Axon Regeneration. Neuron. 2016;92.
12. Kurochkin I, Yonemitsu N, Funahashi S, Nomura H. ALEX1, a novel human armadillo repeat protein that is expressed differentially in normal tissues and carcinomas. Biochem Biophys Res Commun. 2001;280(1):340–7.
13. Iseki H, Takeda A, Andoh T, Takahashi N, Kurochkin I, Yarmishyn A, et al. Human arm protein lost in epithelial cancers, on chromosome X 1 (ALEX1) gene is transcriptionally regulated by CREB and Wnt/beta-catenin signaling. Cancer Sci. 2010;101(6):1361–6.
14. Iseki H, Takeda A, Andoh T, Kuwabara K, Takahashi N, Kurochkin I, et al. ALEX1 suppresses colony formation ability of human colorectal carcinoma cell lines. Cancer Sci. 2012;103(7):1267–71.
15. Gao Y, Wu J, Zeng F, Liu G, Zhang H, Yun H, et al. ALEX1 regulates proliferation and apoptosis in breast Cancer cells. Asian Pac J cancer Prevention: APJCP. 2015;16(8):3293–9.
16. Pang L, Li J, Su L, Zang M, Fan Z, Yu B, et al. ALEX1, a novel tumor suppressor gene, inhibits gastric cancer metastasis via the PAR-1/Rho GTPase signaling pathway. J Gastroenterol. 2018;53(1):71–83.
17. Dang C, O'Donnell K, Zeller K, Nguyen T, Osthus R, Li F. The c-Myc target gene network. Sem Cancer Biol. 2006;16(4):253–64.

18. Dang C. MYC on the path to cancer. Cell. 2012;149(1):22–35.
19. Li M, Yu J, Ju L, Wang Y, Jin W, Zhang R, et al. USP43 stabilizes c-Myc to promote glycolysis and metastasis in bladder cancer. Cell Death Dis. 2024;15(1):44.
20. Wu Z-H, Wang Y-X, Song J-J, Zhao L-Q, Zhai Y-J, Liu Y-F et al. LncRNA SNHG26 promotes gastric cancer progression and metastasis by inducing c-Myc protein translation and an energy metabolism positive feedback loop. Cell Death Dis. 2024;15(3).
21. Zhu Z, Jie W, Fengyu X, Ping H, Yuhang H, Wenfeng Z et al. The m6A modification-mediated positive feedback between glycolytic lncRNA SLC2A1-DT and c-Myc promotes tumorigenesis of hepatocellular carcinoma. Int J Biol Sci. 2024;20.
22. Yu Z, Liting Y, Fang X, Yi H, Yanyan T, Lei S et al. Long non-coding RNA AFAP1-AS1 accelerates lung cancer cells migration and invasion by interacting with SNIP1 to upregulate c-Myc. Signal Transduct Target Ther. 2021;6.
23. Qingqing Z, Chongguo Z, Tianyu Q, Xiyi L, Xuezhi H, Wei L et al. MNX1-AS1 promotes phase separation of IGF2BP1 to Drive c-Myc-mediated cell-cycle progression and proliferation in Lung Cancer. Cancer Res. 2022;82.
24. Kaixin Y, Wenyang Z, Linghui Z, Yinan X, Sudhakar S, Matteo F et al. Long non-coding RNA HIF1A-As2 and MYC form a double-positive feedback loop to promote cell proliferation and metastasis in KRAS-driven non-small cell lung cancer. Cell Death Differ. 2023;30.
25. Farrell A, Sears R. MYC degradation. Cold Spring Harbor Perspect Med. 2014;4(3).
26. Deng L, Meng T, Chen L, Wei W, Wang P. The role of ubiquitination in tumorigenesis and targeted drug discovery. Signal Transduct Target Therapy. 2020;5(1):11.
27. Zhang J, Hu Z, Horta C, Yang J. Regulation of epithelial-mesenchymal transition by tumor microenvironmental signals and its implication in cancer therapeutics. Sem Cancer Biol. 2023;88:46–66.
28. Yuhe H, Weiqi H, Xiawei W. The molecular mechanisms and therapeutic strategies of EMT in tumor progression and metastasis. J Hematol Oncol. 2022;15.
29. Giuseppe B, Sara B, Enrico B, Marco Angelo B, Christian R, Angelo D et al. Epithelial-to-mesenchymal transition in the context of epidermal growth factor receptor inhibition in non-small-cell lung cancer. Biol Rev Camb Philos Soc. 2018;93.
30. Lucas AH, Kristen F, Claudia P. Tumor plasticity and resistance to immunotherapy. Trends Cancer. 2020;6.
31. Davide P, Chiara N, Claudio S, Claudia G. EMT and stemness: flexible processes tuned by alternative splicing in development and cancer progression. Mol Cancer. 2017;16.
32. Rik D, Robert AW. EMT and Cancer: more than meets the Eye. Dev Cell. 2019;49.
33. Montalto F, De Amicis F. Cyclin D1 in Cancer: a molecular connection for cell cycle control, Adhesion and Invasion in Tumor and Stroma. Cells. 2020;9(12).
34. Cunying M, Dandan W, Zhuangfei T, Wenrong G, Yichen Z, Lilin Q et al. USP13 deubiquitinates and stabilizes cyclin D1 to promote gastric cancer cell cycle progression and cell proliferation. Oncogene. 2023;42.
35. Meng F, Hong-Kun W, Yumeng P, Yan Z, Xiangyu G, Yanyun H et al. E3 ligase MG53 suppresses tumor growth by degrading cyclin D1. Signal Transduct Target Ther. 2023;8.
36. Xiaoyun T, Christopher RC, Rongzong L, Roseline G, Basil PH, Todd PWM et al. Lipid phosphate phosphatase-2 promotes tumor growth through increased c-Myc expression. Theranostics. 2022;12.
37. Xinyi Q, Juze Y, Qiongzi Q, Xufan L, Chengxi J, Jia L et al. LCAT3, a novel m6A-regulated long non-coding RNA, plays an oncogenic role in lung cancer via binding with FUBP1 to activate c-MYC. J Hematol Oncol. 2021;14.
38. Zhengguang L, Zhirong Y, Wei L, Wanglong Z, Lan Y, Zhenyu H et al. Dishevleed3 enhanced EMT and cancer stem-like cells properties via Wnt/β-catenin/c-Myc/SOX2 pathway in colorectal cancer. J Transl Med. 2023;21.
39. Iwatsuki M, Mimori K, Ishii H, Yokobori T, Takatsuno Y, Sato T, et al. Loss of FBXW7, a cell cycle regulating gene, in colorectal cancer: clinical significance. Int J Cancer. 2010;126(8):1828–37.
40. Yokobori T, Mimori K, Iwatsuki M, Ishii H, Tanaka F, Sato T, et al. Copy number loss of FBXW7 is related to gene expression and poor prognosis in esophageal squamous cell carcinoma. Int J Oncol. 2012;41(1):253–9.
41. Imura S, Tovuu L, Utsunomiya T, Morine Y, Ikemoto T, Arakawa Y, et al. Role of Fbxw7 expression in hepatocellular carcinoma and adjacent non-tumor liver tissue. J Gastroenterol Hepatol. 2014;29(10):1822–9.
42. Yokobori T, Yokoyama Y, Mogi A, Endoh H, Altan B, Kosaka T, et al. FBXW7 mediates chemotherapeutic sensitivity and prognosis in NSCLCs. Mol cancer Research: MCR. 2014;12(1):32–7.
43. Wei G, Wang Y, Zhang P, Lu J, Mao J. Evaluating the prognostic significance of FBXW7 expression level in human breast cancer by a meta-analysis of transcriptional profiles. J cancer Sci Therapy. 2012;4(9):299–305.
44. Welcker M, Orian A, Jin J, Grim J, Harper J, Eisenman R, et al. The Fbw7 tumor suppressor regulates glycogen synthase kinase 3 phosphorylation-dependent c-Myc protein degradation. Proc Natl Acad Sci USA. 2004;101(24):9085–90.
45. Zhang Z, Xu P, Hu Z, Fu Z, Deng T, Deng X, et al. CCDC65, a Gene Knockout that leads to early death of mice, acts as a potentially novel tumor suppressor in Lung Adenocarcinoma. Int J Biol Sci. 2022;18(10):4171–86.


## Publisher's note